WILEY

IL-17A-producing T cells exacerbate fine particulate matter-induced lung inflammation and fibrosis by inhibiting PI3K/Akt/mTOR-mediated autophagy

Lu-Hong Cong[1] | Tao Li[2] | Hui Wang[2] | Yi-Na Wu[2] | Shu-Peng Wang[2] |
Yu-Yue Zhao[2] | Guo-Qiang Zhang[1] | Jun Duan[2] 🆔

[1]Department of Emergency, China-Japan Friendship Hospital, Beijing, China

[2]Surgical Intensive Care Unit, China-Japan Friendship Hospital, Beijing, China

Correspondence
Jun Duan, Surgical Intensive Care Unit, China-Japan Friendship Hospital, No. 2, Yinghua East Street, Chaoyang District, Beijing 100029, China.
Email: dj_mail2000@163.com

Abstract

Fine particulate matter (PM2.5) is the primary air pollutant that is able to induce airway injury. Compelling evidence has shown the involvement of IL-17A in lung injury, while its contribution to PM2.5-induced lung injury remains largely unknown. Here, we probed into the possible role of IL-17A in mouse models of PM2.5-induced lung injury. Mice were instilled with PM2.5 to construct a lung injury model. Flow cytometry was carried out to isolate $\gamma\delta$T and Th17 cells. ELISA was adopted to detect the expression of inflammatory factors in the supernatant of lavage fluid. Primary bronchial epithelial cells (mBECs) were extracted, and the expression of TGF signalling pathway-, autophagy- and PI3K/Akt/mTOR signalling pathway-related proteins in mBECs was detected by immunofluorescence assay and Western blot analysis. The mitochondrial function was also evaluated. PM2.5 aggravated the inflammatory response through enhancing the secretion of IL-17A by $\gamma\delta$T/Th17 cells. Meanwhile, PM2.5 activated the TGF signalling pathway and induced EMT progression in bronchial epithelial cells, thereby contributing to pulmonary fibrosis. Besides, PM2.5 suppressed autophagy of bronchial epithelial cells by up-regulating IL-17A, which in turn activated the PI3K/Akt/mTOR signalling pathway. Furthermore, IL-17A impaired the energy metabolism of airway epithelial cells in the PM2.5-induced models. This study suggested that PM2.5 could inhibit autophagy of bronchial epithelial cells and promote pulmonary inflammation and fibrosis by inducing the secretion of IL-17A in $\gamma\delta$T and Th17 cells and regulating the PI3K/Akt/mTOR signalling pathway.

KEYWORDS
autophagy, IL-17A, lung injury, PI3K/Akt/mTOR signalling pathway, PM2.5, pulmonary fibrosis, pulmonary inflammatory response

1 | INTRODUCTION

Lung injury can contribute to a pulmonary inflammatory response and breathing pattern changes.[1] Lung inflammation is featured by elevated depletion of pulmonary inflammatory cells and the secretion of pro-inflammatory mediators, which results in the protein leakage in alveolar space and decrease in lung compliance and lung function impairment.[2] Despite the reduction in mortality due to improved supportive care such as conservative fluid strategy and lung protective ventilation, the overall rate of mortality in lung injuries remains very high.[3] Until now, there are no pharmacological therapies for the improvement of the clinical outcomes in lung injury,[4] which underscores the necessity for novel therapeutic strategies against lung injury.

Ambient air pollution, especially the environmental particulate matter (PM), has increasingly become a main public health issue in China. Inhalation of fine particulate matter (PM2.5) with a diameter of <2.5 μm can induce both inflammation of the airways and systemic inflammation.[5] Some studies have suggested that exposure to PM2.5 is related to reduced lung function and increased incidences of airway ailments, including asthma, acute airway inflammation, allergic airway disease and chronic obstructive pulmonary disease (COPD).[6,7]

Pulmonary fibrosis is a chronic diffuse lung disease which is featured by progressive deterioration of lung function ultimately resulting in death.[8] It is suggested to be a result of an ongoing lung injury happening at discrete sites over a period of time.[9] Severe lung injury-induced pulmonary fibrosis results from diverse aetiological factors (lipopolysaccharide [LPS], severe acute respiratory syndrome-associated coronavirus [SARS-CoV], avian influenza A [H5N1]-virus) and some other unknown factors.[10]

Interleukin (IL)-17A, a glycoprotein secreted by IL-17-producing cells, is found to be a pro-inflammatory cytokine participating in both chronic inflammation and autoimmune diseases.[11] IL-17A has been found to participate in pulmonary fibrosis depending on transforming growth factor (TGF)-β1, and the constituents of the IL-17A signalling pathway are potent therapeutic targets for the treatment of fibroproliferative lung diseases.[11] TGF-β is a multifunctional cytokine, which plays a major role in the pathogenesis of several human diseases including pulmonary fibrosis.[12] Meanwhile, pulmonary fibrosis has been suggested to be accompanied by autophagy, and the levels of autophagy proteins are enhanced in both COPD and asthma patients.[13] In addition, it has been reported that PM2.5 inhibits autophagy of bronchial epithelial cells by activating the phosphatidylinositol-3-kinase (PI3K)/protein kinase B (Akt) and the mammalian target of rapamycin (mTOR) signalling pathway.[14] Moreover, another report also confirmed that IL-17A can inhibit autophagy in keratinocytes by activating the PI3K/Akt/mTOR signalling pathway.[15] In our study, we have found out that PM2.5 could suppress autophagy to induce pulmonary inflammatory response and fibrosis by inducing the secretion of IL-17A via the PI3K/Akt/mTOR signalling pathway.

2 | MATERIALS AND METHODS

2.1 | Ethics statement

All the animals were treated and cared for in humane situation, in line with the guide prepared by the Committee of the Care and Use of Laboratory Animals of China-Japan Friendship Hospital. All efforts were made to minimize the number and suffering of the included animals.

2.2 | Establishment of PM2.5-induced mouse models

PM2.5 was collected as per the previously described method.[16] Briefly, PM2.5 was collected in Beijing from 2017 to 2018 by a PM2.5 high volume sampler system (Staplex® No PM-2.5 SSI). With an air flow rate of 1.13 m³/min, the filter paper (20.3 × 25.4 cm) was utilized to collect PM2.5. Next, the filters were dried at 50°C for 24 hours and weighed on a high-precision microbalance before and after PM collection. The filters with PM2.5 were cut into 1 × 3 cm small pieces and then sonicated in sterile distilled water for 2 hours to remove PM2.5 from the filters. The water for extracting PM2.5 was next centrifuged at 5000 × g and 4°C and weighed after vacuum freeze drying. Subsequently, the extracted particles were weighed and stored at −20°C. PM2.5 suspension solution was always treated by sonication and vortex before experiment.[16-18]

Male C57BL/6J mice (n = 30, aged 6-7 weeks, weighing 20-30 g) were purchased from Beijing Vital River Laboratory Animal Technology Co., Ltd. IL-17A knockout (IL-17A⁻/⁻) C57BL/6J mice (n = 15) were purchased from Cyagen Biosciences Inc (Guangzhou, China; KOCMP-21005-Il17a). The mouse model establishment and breeding were performed as described previously in literature.[19-21] The mice were housed in a specific pathogen-free animal room and kept at 22-25°C under 60%-65% humidity. All mice were given ad libitum access to water and food. The mice in the experimental group (15 IL-17A wild type [WT] mice and 15 IL-17A⁻/⁻ mice) were subjected to intratracheal instillation of 2 mg/mL PM2.5 using normal saline. The model construction lasted for 9 days, during which the intratracheal instillation was performed once every 3 days, 50 μL for each mouse. Five mice in the control, WT and IL-17A⁻/⁻ groups were, respectively, euthanized on the 3rd, 6th and 9th day of model construction. Next, lung tissue and alveolar lavage fluid were extracted for subsequent experiments.

2.3 | Extraction and culture of primary mouse tracheal epithelial cells

Bronchial rings were isolated from mouse lung tissue, washed with pre-chilled phosphate-buffered saline (PBS) and incubated in minimal essential medium (MEM, 11095-080, Fisher Scientific

International) containing 1.4 mg/mL pronase and 0.1 mg/mL DNase (Roche Diagnostics) for 16 hours at 4°C. After that, the undigested excess tissue was removed using a 100-mesh cell sieve (YA0945-100 mesh, Beijing Solarbio Science & Technology Co., Ltd.). Collagenase was neutralized using MEM containing 10% foetal bovine serum (FBS, ExCell Bio, Genetimes). The supernatant was discarded after centrifugation at 800 × g for 5 minutes, and the cells were resuspended in MEM containing 10% FBS and then seeded in a culture flask. Subsequently, the culture medium (including the suspended cells therein) was collected, and the supernatant was removed after centrifugation at 800 × g for 5 minutes. The bronchial epithelial cells were next cultured using bronchial epithelial growth medium (BEGM, CC-3170, BioWhittaker).

For virus infection, 4×10^5 bronchial epithelial cells were first seeded in 6-well plates. After incubation for 24 hours in Dulbecco's modified Eagle's medium (DMEM) containing 10% FBS, 1 μL adenovirus working solution (1×10^8 pfu/mL) containing adenovirus negative control (Ad-NC) or Ad-IL-17A adenoviruses (GenePharma) was added to the medium. To inhibit TGF-β1, bronchial epithelial cells were treated with 10 μmol/L TGF-β1 inhibitor, LY3200882 (S8772, Selleck Chemicals) for 24 hours.

2.4 | Haematoxylin-eosin (HE) staining

The lung tissues were fixed in 4% paraformaldehyde solution (P0099, Beyotime) for 24 hours and then dehydrated in conventional method using a gradient of different alcohol concentrations (70%, 80%, 90%, 95%, 100). Next, the tissues were permeabilized twice with xylene (10 minutes each), embedded by paraffin and cut into 4-μm-thick sections. Afterwards, the tissue sections were deparaffinized with xylene, stained with haematoxylin for 10 minutes and incubated in 1% hydrochloric acid alcohol for 20 seconds. After treated with 1% ammonia water, the tissue sections were stained with eosin for 3 minutes, dehydrated by gradient ethanol, permeabilized by xylene and then sealed by neutral balsam. The morphological observation of lung tissues was conducted under an ordinary optical microscope (40×, Olympus).

2.5 | Masson staining

After dewaxing, the sections were stained with Ponceau S staining solution for 2 minutes. This was followed by treatment with 0.2% glacial acetic acid solution for 2 minutes, 5% molybdophosphoric acid solution for 2 minutes, 0.2% glacial acetic acid solution for 2 minutes and Methyl Green staining solution for 3 minutes, respectively. The sections were then washed, differentiated with 95% alcohol, dehydrated with alcohol, permeabilized by xylene and lastly sealed by neutral balsam. Under an optical microscope with 100× magnification, the deformed area of collagen-rich fibres was stained blue and the cellular matrix was stained red. A total of 10 visual fields were randomly selected from each section for imaging. The images

TABLE 1 The primer sequences for RT-qPCR

Gene	Primer sequence (5′-3′)
IL-1β	F: 5′-AAACAGATGAAGTGCTCCTTCCAGG-3′
	R: 5′-TGGAGAACACCACTTGTTGCTCCA-3′
IL-17A	F: 5′-TTTAACTCCCTTGCGCAAAA-3′
	R: 5′-CTTTCCCTCCGCATTGACAC-3′
TNF-α	F: 5′-CGAGTGACAAGCCCGTAGCC-3′
	R: 5′-GGATGAACACGCCAGTGGCC-3′
TGF-β1	F: 5′-ATTCCTGGCGTTACCTTGG-3′
	R: 5′-AGCCCTGTATTCCGTCTCCT-3′
α-SMA	F: 5′-TGCTGACAGAGGCACCACTGAA-3′
	R: 5′-CAGTTGTACGTCCAGAGGCATA-3′
GAPDH	F: 5′-ACTTGAAGGGTGGAGCCAAA-3′
	R: 5′-GTGGTCATGAGCCCTTCCAC-3′

Note: F, forward; R, reverse; RT-qPCR, reverse transcription quantitative polymerase chain reaction; IL, interleukin; TNF-α, tumour necrosis factor-α; TGF-β1, transforming growth factor-beta; α-SMA, alpha smooth muscle actin; GAPDH, glyceraldehyde-3-phosphate dehydrogenase.

were collected and analysed by ImageJ software. The degree of liver fibrosis was expressed as the percentage of area with fibrosis in the whole area.

2.6 | Reverse transcription quantitative polymerase chain reaction (RT-qPCR)

The total RNA was extracted using TRIzol (Invitrogen). The reverse transcription of first strand complementary DNA (cDNA) was performed with the First Strand cDNA Synthesis Kit (Takara Bio) according to instructions. The PCR was conducted using SYBR Premix Ex Taq kit (Takara Bio) in ABI Prism 7500 Fast Real-Time PCR system (Applied Biosystems). Glyceraldehyde-3-phosphate dehydrogenase (GAPDH) was used as the internal reference. The primers are listed in Table 1. The relative expression was analysed by $2^{-\Delta\Delta Ct}$ method.

2.7 | Western blot analysis

The protein was extracted using radioimmunoprecipitation assay lysis buffer (R0010, Beijing Solarbio Science & Technology Co., Ltd.), and the total protein concentration was measured using bicinchoninic acid kit (P0011, Beijing Solarbio Science & Technology Co., Ltd.) as per the instructions. The extracted proteins were then separated by polyacrylamide gel electrophoresis. Subsequently, the proteins were transferred to a 0.2 μm polyvinylidene difluoride membrane (ISEQ10100, Millipore). The membrane was blocked with Tris-buffered saline-0.1% Tween-20 (TBST) solution (D8340, Beijing Solarbio Science & Technology Co., Ltd.) containing 5% skimmed milk for 1 hour and the incubated with primary antibody at 4°C overnight. The membrane was then incubated with horseradish

peroxidase (HRP)-labelled goat anti-rabbit immunoglobulin G (IgG) (1:5000, A0208, Beyotime) for 1 hour at room temperature. The digital chemiluminescence instrument (C-DiGit® Blot Scanner, Li-Cor) was used to visualize immunocomplexes on the membranes and Image J software (US National Institutes of Health) was used to measure band intensities. The relative protein expression was calculated as a ratio of the grey value of target bands to that of GAPDH. The primary antibodies used in the experiment included rabbit polyclonal antibody against p-smad2 (Ser465/467)/smad3 (Ser423/425) (#8828), smad2/smad3 (#8685), alpha smooth muscle actin (α-SMA) (#19245), E-cadherin (#3195), Snail (#3879), p-PI3K (Tyr458/Tyr199) (#4228), PI3K (#4257), p-Akt (Ser473) (#4058), Akt (#4685), p-mTOR (Ser2448) (#5536), mTOR (#2983), LC3 (#4108), DRP1 (#5391), MFN2 (#11925), TOM20 (#42406) (all 1:1000, Cell Signaling Technology), type I Collagen (1:1000, ab34710, Abcam), ZO-1 (1:1000, 21773-1-AP, Proteintech), and GAPDH (1:4000, 10494-1-AP, Proteintech).

The cells were harvested and centrifuged at 800 × *g* for 5 minutes at 4°C. After the supernatant was discarded, the pellet was incubated with 1-2.5 mL mitochondrial separation reagent (C3601, Beyotime) in an ice bath for 10-15 minutes. Next, the cell suspension was transferred to a suitably sized glass homogenizer and homogenized for about 10-30 times. The cell homogenate was centrifuged at 600 × *g* for 10 minutes at 4°C, after which the supernatant was carefully transferred to another centrifuge tube and centrifuged at 11 000 × *g* for 10 minutes at 4°C. After the supernatant was discarded, the precipitate was the isolated mitochondria. The protein analysis of mitochondria was similar to the above-described methods.

2.8 | Immunofluorescence assay

The cells were cultured in a culture dish (NEST Biotechnology Co.) to allow imaging using a confocal microscope. Cells were fixed by 4% paraformaldehyde for 30 minutes, washed gently thrice with 1 × PBS and penetrated with 1 × PBS containing 0.1% Triton X-100 for 5 minutes at room temperature. Then, the cells were blocked in 1 × PBS containing 5% bovine serum albumin (BSA) for 30 minutes at room temperature followed by overnight incubation with the primary antibody at 4°C. The next day, the cells were incubated with fluorescein-labelled secondary antibody (1:50, Dianova) under dark conditions for 45 minutes. Then, the cell nuclei were stained with 4,6-diamidino-2-phenylindole (DAPI) for 30 minutes under dark conditions. Subsequently, the cells were covered by anti-fluorescent quencher and observed under a laser confocal scanning microscope (SP8, Leica) at an excitation wavelength of 488 nm. The secondary antibody was goat anti-rabbit iFluor™ 488IgG (16 608, AAT Bioquest). The cells were isolated and cultured to a certain density in a culture dish. After removing the culture medium, the cells were incubated with Mito-Tracker Red CMX Ros working solution (C1049-50 μg, Beyotime) at 37°C for 30 minutes. The Mito-Tracker Red CMXRos working solution

was removed, and pre-incubated DMEM was added. Finally, the mitochondria were observed under a laser confocal scanning microscope (SP8, Leica) at 594 nm.

2.9 | Flow cytometry

As previously described,[22] the cells were detached from the lung tissue by incubation in Roswell Park Memorial Institute (RPMI) 1640 medium (11875093, Invitrogen) containing 2 mg/mL collagenase type XI (Sigma-Aldrich) and 100 g/mL DNase I (Sigma-Aldrich) for 1 hour at 37°C, and 2 mmol/L ethylene diamine tetraacetic acid was added 5 minutes before the end of the detachment. Next, the detachment was terminated using RPMI 1640 medium containing 10% FBS and undetached excess tissue was removed using a 100-mesh cell sieve (YA0945-100 mesh, Solarbio). After centrifugation at 800 × *g* for 5 minutes, the supernatant was discarded and the cells were resuspended using RPMI 1640 medium containing 10% FBS. The cells were further purified using 35% Percoll (Sigma-Aldrich) density gradient centrifugation, and red blood cells were removed.

For flow cytometry, 1×10^6 cells were incubated with fluorescent labelling membrane protein antibody diluted 1:10 with 5% BSA at 4°C for 20 minutes. Subsequently, the cells were fixed in 4% paraformaldehyde, permeabilized using 0.05% Trizon-100 and incubated with APC-labelled IL-17A monoclonal antibody (17-7177-81, eBioscience™, Invitrogen) diluted 1:10 with 5% BSA. After three washes using PBS, the cells were detected using a LSR II flow cytometer (BD Biosciences). Membrane protein antibody used included: fluorescein isothiocyanate (FITC)-labelled CD3 monoclonal antibody (1:10, 11-0031-82, eBioscience™), phycoerythrin (PE)-labelled CD4 monoclonal antibody (1:10, 12-0041-82, eBioscience™) and PE-labelled TCR γδ monoclonal antibody (1:10, 12-5711-82, eBioscience™).

2.10 | Detection of bronchoalveolar lavage fluid

The mice were anesthetized by intraperitoneal injections of 0.05 mg pentobarbital sodium (P3761, Sigma-Aldrich) per 1 g of body weight. The lavage fluid was made using sterile 1 × PBS containing 1% BSA and 5000 IU/l heparin. The trachea was cannulated, and the mouse bronchi were rinsed with lavage fluid and washed thrice with the fluid collected. The supernatant was harvested after centrifugation at 800 × *g* for 5 minutes. Cells were resuspended in 1 × PBS, and the immune cells were distinguished with Wright-Giemsa stain (DM0007, Leagene Biotechology).

2.11 | Enzyme-linked immunosorbent assay (elisa)

After collecting the alveolar lavage fluid, ELISA were performed according to the instructions for IL-17A, tumour necrosis factor-α

(TNF-α) and IL-1β ELISA kits (H052 and H002, Nanjing Jiancheng Bioengineering institute). The antigen was solubilized in 50 mmol/L carbonate coating buffer (pH 9.6) to get an antigen concentration of 10-20 µg/mL, and each well of the 96-well microtitre plate was coated with 100 µL antigen solution at 4°C overnight. The coating buffer was discarded and each well was blocked for 1 hour with 50 µL 1% BSA at 37°C, followed by incubation with 100 µL of lavage solution with different dilutions at 37°C for 2 hours. Next, each well was incubated for 1 hour with 100 µL diluted HRP-labelled secondary antibody at 37°C and then developed for 20 minutes. The absorbance at A405 was read using a microplate reader (BioTek ELx800, BioTek).

2.12 | Cellular reactive oxygen species (ROS) detection

Cellular ROS in cells was detected using ROS detection kit (S0033, Beyotime) as per the instructions. Briefly, (2′,7′-dichlorodihydrofluorescin diacetate (DCFH-DA) was diluted with MEM to a final concentration of 10 µmol/L. The cells were collected and suspended in diluted DCFH-DA at a concentration of 1×10^6 cells/mL and incubated in a 37°C cell incubator for 20 minutes. The cells were washed thrice with MEM to remove DCFH-DA that did not enter the cells. The ROS was detected at an excitation wavelength of 488 nm and an emission wavelength of 525 nm using a LSR II flow cytometer (BD Biosciences).

2.13 | Cellular adenosine triphosphate (ATP) content detection

Cells at a density of 1×10^4 cells/well were seeded in a 96-well plate with 100 µL medium per well. Then, 100 µL CellTiter-Glo® Reagent (CellTiter-Glo® Luminescent Cell Viability Assay, G7570, Promega) was added to each well and cells were lysed for 2 minutes under dark conditions. The supernatant was transferred to an opaque 96-well plate and the signal was measured with a GloMax® 96 Microplate Luminometer (GloMaxTM, Promega).

2.14 | Statistical analysis

The data were analysed using SPSS 21.0 statistical software (IBM Corp.). Data from at least three independent experiments were used to represent all the results in this study. Measurement data were expressed as mean ± standard deviation. Normally distributed data between two groups were compared using t test while those among multiple groups were analysed using one-way analysis of variance (ANOVA), followed by Tukey's post hoc test. $P < .05$ indicated that the difference was of statistical significance.

3 | RESULTS

3.1 | PM2.5 treatment increased the number of γδT and Th17 cells

Lung tissues of mice were examined to investigate the effect of PM2.5 exposure on inflammation and immune cell accumulation. In WT mice following PM2.5 treatment, HE staining revealed lung tissues infiltrated with a large number of inflammatory cells (Figure 1A). Meanwhile, investigation of alveolar lavage fluid showed an increased number of whole cells after PM2.5 induction, along with significant increase in neutrophils ($P < .05$, Figure 1B). At the 3rd, 6th and 9th days post-model establishment, the number of γδT and Th17 cells showed no changes in the lung tissues of control mice ($P > .05$, Fig. C, E and F) while a gradual increase was observed in the lung tissues of PM2.5-treated mice ($P < .05$, Figure 1D-F).

3.2 | PM2.5 treatment promoted IL-17A secretion by γδT/Th17 cells and aggravated inflammatory response

Both γδT and Th17 cells have been reported to secrete IL-17. Thus, we employed RT-qPCR to determine the mRNA expression of Th17 at the 3rd, 6th and 9th days of PM2.5-induced model establishment and found a gradual increase in Th17 mRNA expression ($P < .05$, Figure 2A). The expression of inflammatory factors IL-1β and TNF-α in the supernatant of alveolar lavage fluid was detected by ELISA, which suggested that the levels of IL-17A, IL-1β and TNF-α were significantly increased after 9 days of PM2.5-induced model establishment ($P < .05$, Figure 2B, C). The mRNA expression of TNF-α and IL-1β was also detected by RT-qPCR, which confirmed ELISA results ($P < .05$, Figure 2D). Further study in IL-17A$^{-/-}$ mice revealed that knockout of IL-17A could reduce inflammatory cell infiltration in lung tissues at the 9th day of PM2.5-induced model establishment (Figure 2E). Compared with WT mice, IL-17A$^{-/-}$ mice presented with decreased expression of IL-1β and TNF-α in the alveolar lavage supernatant (Figure 2F), decreased number of neutrophils (Figure 2G) and mRNA expression of TNF-α and IL-1β (Figure 2H) (all $P < .05$) after 9 days of PM2.5-induced model establishment. The aforementioned results suggested that PM2.5 could aggravate inflammatory response by promoting the secretion of IL-17A by γδT/Th17 cells.

3.3 | PM2.5 treatment triggered an increase in IL-17A secretion and activated the TGF signalling pathway

We next intended to explore the involvement of the fibrosis-related signalling pathways in the lung injury caused by PM2.5. Firstly, we examined the expression of SMAD family of proteins in the TGF-β signalling pathway. After 9 days of PM2.5-induced model
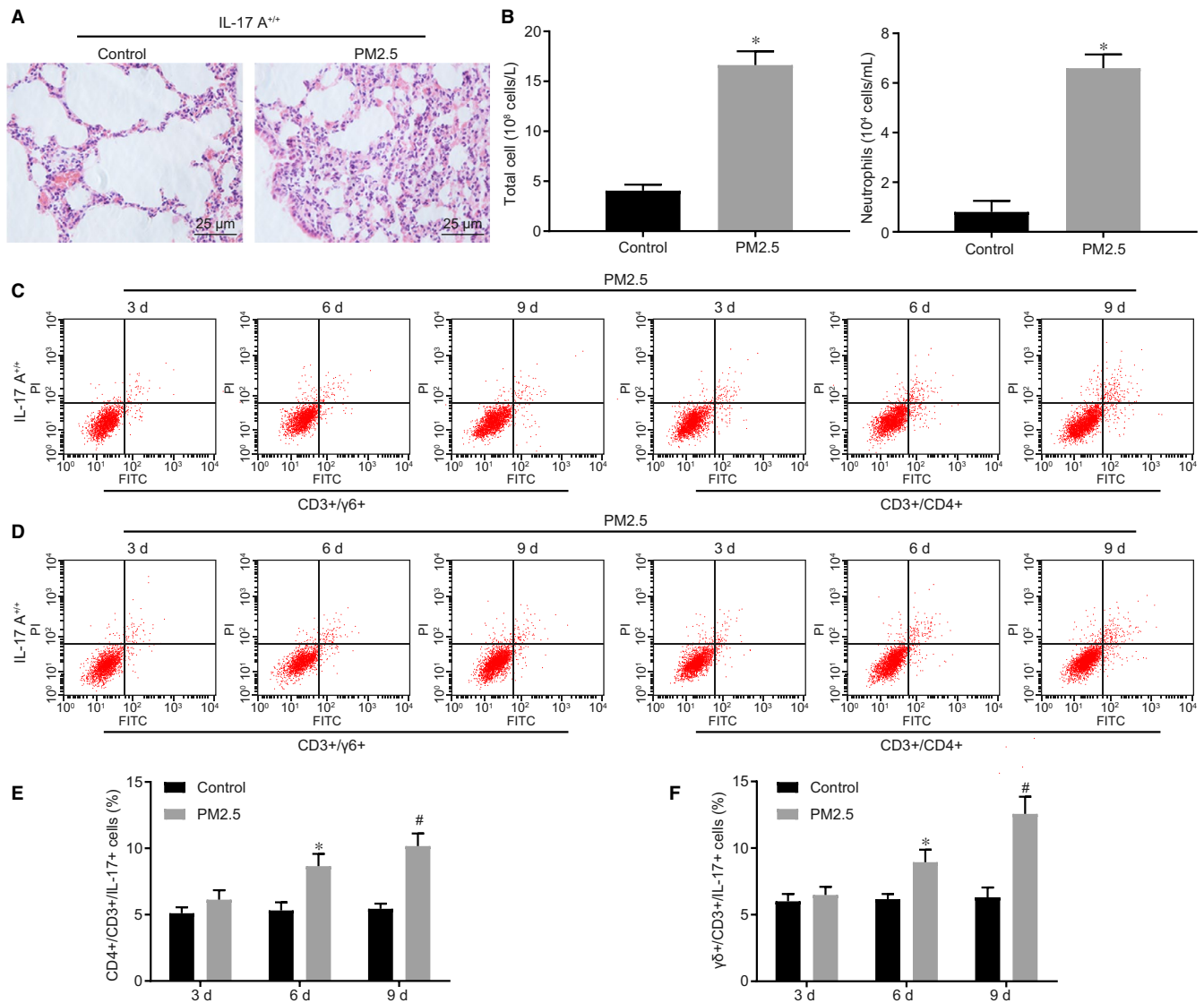
FIGURE 1 PM2.5 treatment increases γδT and Th17 cells. A, HE staining analysis of mouse lung tissues (n = 5 for each group) (×400). B, Analysis of alveolar lavage fluid, the left panel shows the number of total cells, and the right panel shows the number of neutrophils. *P < .05 vs control mice (n = 5 for each group). C-F, The number of IL-17A$^+$ cells at the 3rd, 6th and 9th days of model establishment analysed by flow cytometry. *P < .05 vs the 3rd day, #P < .05 vs the 6th day (n = 5 for each group). Data (mean ± standard deviation) between two groups were compared using t test and those among multiple groups were assessed by one-way ANOVA with Tukey's post hoc test. Cell experiment was repeated 3 times

establishment, WT mice exhibited increased collagen deposition in lung tissue (Figure 3A), augmented mRNA expression of TGF-β1, COL1A1 and α-SMA (Figure 3B), and elevated phosphorylation levels of SMAD2 and SMAD3 (Figure 3C) (all P < .05), all of which indicated that PM2.5 stimulation promoted activation of the TGF-β signalling pathway in WT mice. There was no significant change in the fibrosis indexes between the IL-17A$^{+/+}$ and IL-17A$^{-/-}$ mice without PM2.5 treatment (Figure 3A-C). However, knockout of IL-17A reduced collagen deposition and TGF-β1 secretion, inhibited the phosphorylation levels of SMAD2 and SMAD3, along with COL1A1 and α-SMA expression in PM2.5-induced mouse models (Figure 3A, B), which were indicatives of alleviated lung tissue fibrosis. Therefore, PM2.5 treatment could enhance IL-17A secretion and activate the TGF signalling pathway.

3.4 | PM2.5 treatment accelerated IL-17A secretion leading to pulmonary fibrosis via activation of the TGF signalling pathway

Further, the primary bronchial epithelial cells were extracted from WT and IL-17A$^{-/-}$ mice. The results showed that the phosphorylation levels of SMAD2 and SMAD3, expression of α-SMA and Snail were increased (Figure 4A, B), while the expression of E-cadherin and ZO-1 was decreased in cells (Figure 4A) after 9 days of PM2.5-induced model establishment (all P < .05), indicating that epithelial-mesenchymal transition (EMT) occurred in bronchial epithelial cells under PM2.5 stimulation. IL-17A$^{-/-}$ mice treated with PM2.5 had reduced collagen deposition (Figure 3A) and TGF-β1 and α-SMA mRNA expression (Figure 3B), inhibited phosphorylation levels
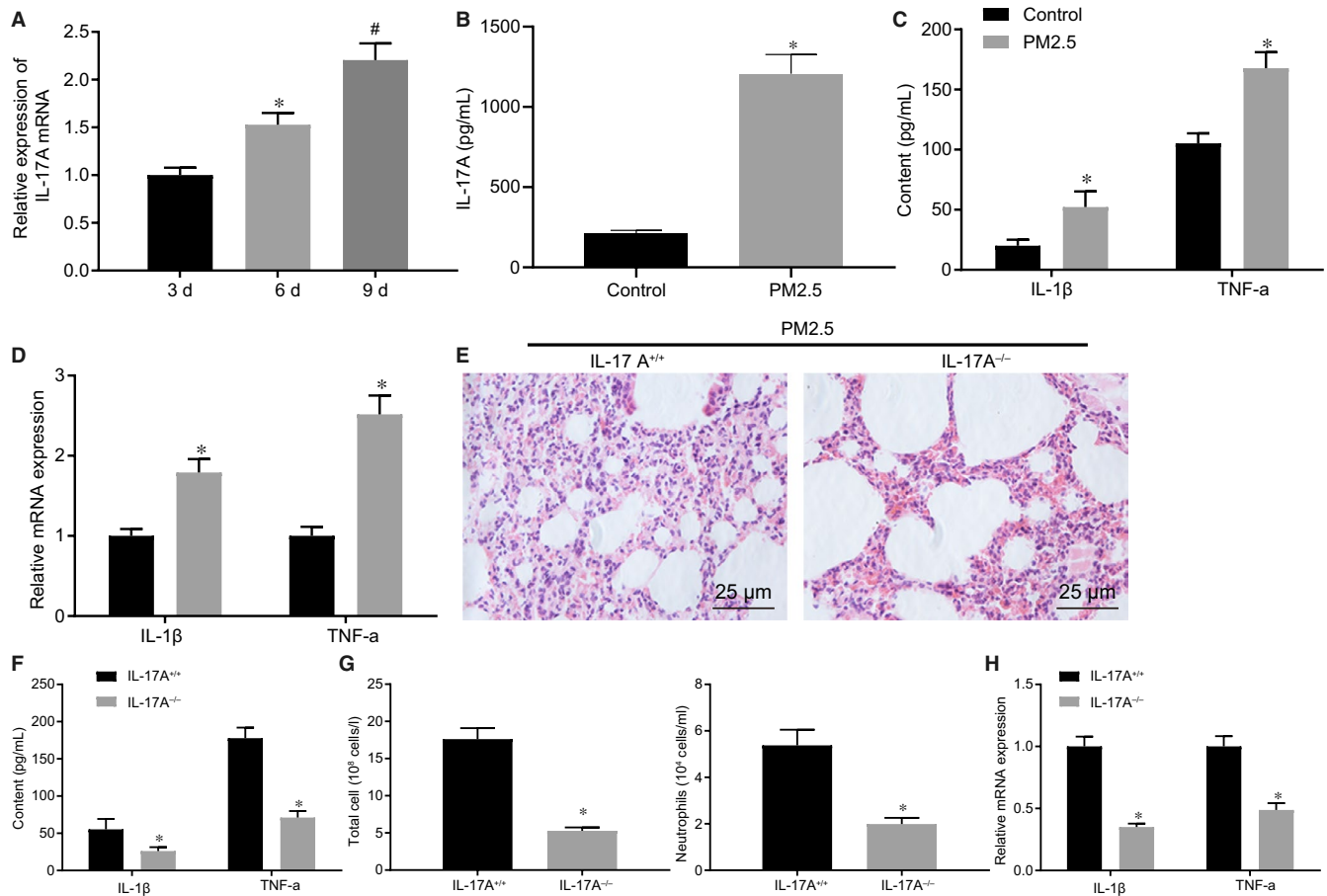
FIGURE 2 PM2.5 treatment aggravates inflammatory response by promoting the secretion of IL-17A by γδT/Th17 cells. A, IL-17A mRNA expression in PM2.5-treated mice detected by RT-qPCR. B, IL-17A expression in the supernatant of alveolar lavage fluid of PM2.5-treated mice measured by ELISA. C, The expression of IL-1β and TNF-α in the supernatant of alveolar lavage fluid of PM2.5-treated mice detected by ELISA. D, The expression of TNF-α and IL-1β in PM2.5-treated mice detected by RT-qPCR. In panel A-D, *P < .05 vs control mice. E, HE staining analysis of lung tissues of IL-17A$^{-/-}$ mice (×400). F, The expression of IL-1β and TNF-α in the supernatant of alveolar lavage fluid of IL-17A$^{-/-}$ mice detected by ELISA. G, Detection results of alveolar lavage fluid. The left panel shows the number of total cells, and the right panel shows the number of neutrophils. H, The expression of TNF-α and IL-1β in IL-17A$^{-/-}$ mice detected by RT-qPCR. In panel E-H, * P < .05 vs IL-17A$^{+/+}$ mice. n = 5 for each group. Data (mean ± standard deviation) between two groups were compared using t test and those among multiple groups were assessed by one-way ANOVA with Tukey's post hoc test. Cell experiment was repeated 3 times

of SMAD2 and SMAD3, along with COL1A1 and α-SMA expression compared to WT mice (all P < .05) (Figure 3C). After 9 days of PM2.5-induced model establishment, the phosphorylation levels of SMAD2 and SMAD3, as well as the expression of α-SMA and Snail were lower (Figure 4A), and E-cadherin and ZO-1 expression was higher in cells from IL-17A$^{-/-}$ mice than from WT mice (all P < .05) (Figure 4A, B). Meanwhile, we treated primary bronchial epithelial cells with LY3200882, TGF-β1 inhibitor, which suggested that the treatment of LY3200882 reduced the phosphorylation levels of SMAD2 and SMAD3 and expression of α-SMA, and increased the expression of E-cadherin induced by PM2.5 (all P < .05, Figure 4C). However, overexpression of IL-17A reduced E-cadherin expression and elevated α-SMA expression in cells of IL-17A$^{-/-}$ mice (P < .05, Figure 4D, E). These results suggested that PM2.5 promoted the secretion of IL-17A, activated the TGF signalling pathway and induced EMT in bronchial epithelial cells, thereby leading to pulmonary fibrosis.

3.5 | PM2.5 treatment inhibited cell autophagy by activating the PI3K/AKT/MTOR signalling pathway in bronchial epithelial cells by promoting IL-17A expression

Next, we attempted to further clarify how PM2.5 affected the function of bronchial epithelial cells. After PM2.5-induced model establishment, the expression of LC3 II (Figure 5A, B) was increased and the expression of p62 (Figure 5B) was decreased in bronchial epithelial cells of IL-17A$^{-/-}$ mice compared to WT mice (both P < .05), suggesting that PM2.5 treatment could block autophagy of bronchial epithelial cells. Furthermore, the phosphorylation levels of PI3K, Akt, and mTOR were increased in the bronchial epithelial cells from IL-17A$^{-/-}$ mice compared to WT mice (all P < .05, Figure 5C), indicating that PM2.5 could activate PI3K/Akt/mTOR signalling pathway. Furthermore, IL-17A$^{-/-}$ mice following PM2.5 treatment showed down-regulated p62 expression
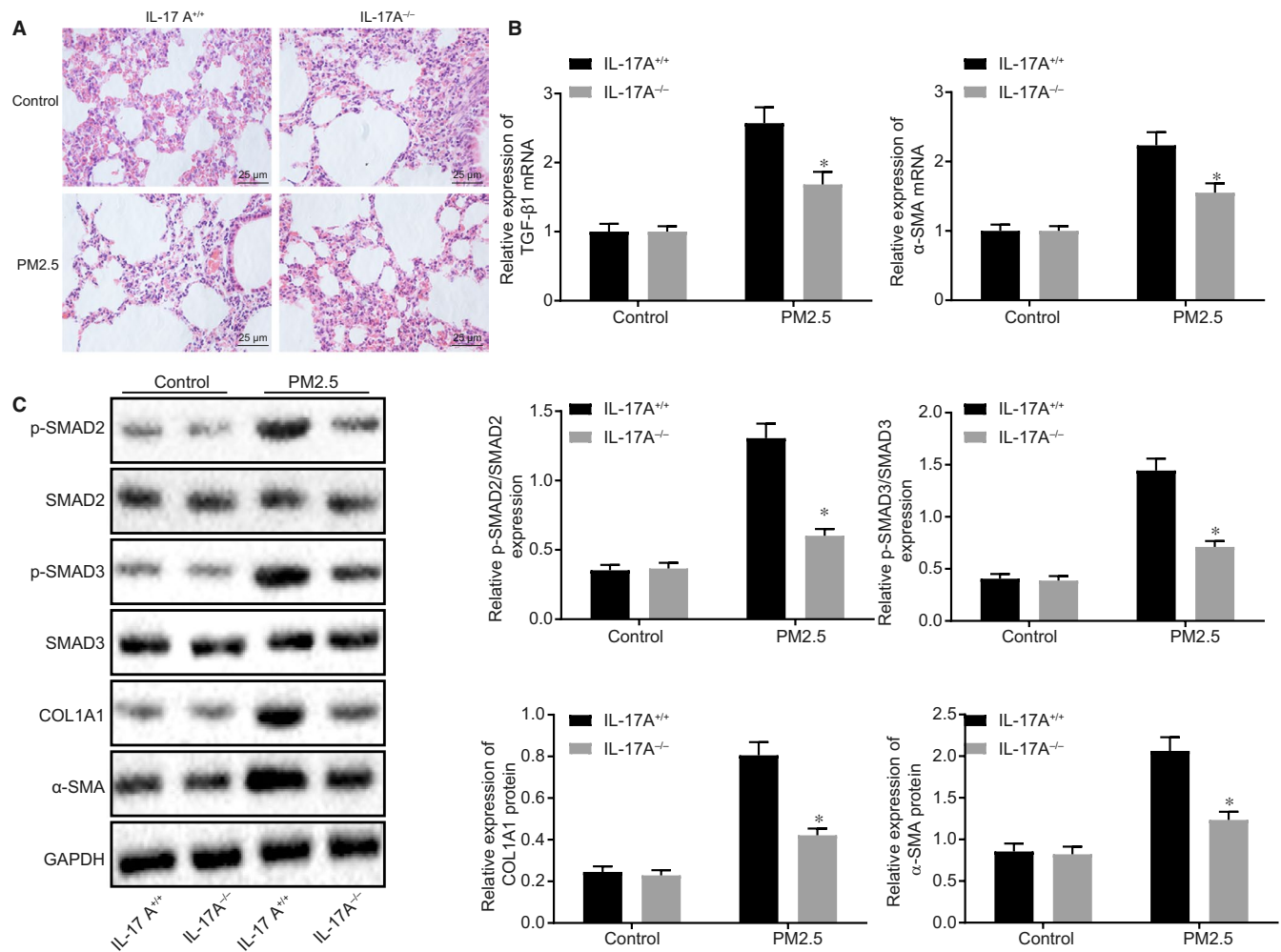
FIGURE 3 PM2.5 treatment promotes IL-17A secretion and then activates the TGF signalling pathway. A, Masson staining of collagen deposition in mouse lung tissues (×400). B, TGF-β1 and α-SMA mRNA expression in mouse lung tissues detected by RT-qPCR. C, Western blot analysis of SMAD2, p-SMAD2, SMAD3, p-SMAD3, COL1A1 and α-SMA proteins in mouse lung tissues. The left panel represents representative protein bands, and the right panels represent statistical charts. *$P < .05$ vs IL-17A$^{+/+}$ mice following PM2.5 treatment. n = 5 for each group. Data (mean ± standard deviation) between two groups were compared using t test and those among multiple groups were assessed by one-way ANOVA with Tukey's post hoc test. Cell experiment was repeated 3 times

and mTOR phosphorylation level while LC3 expression was up-regulated ($P < .05$, Figure 5D, E), confirming that PM2.5 inhibited autophagy and activated mTOR signalling pathway in bronchial epithelial cells, which was dependent on IL-17A. In addition, starving cells are commonly used to study autophagy.[11] By promoting the autophagy level of cells in each group, the effect of IL-17A knock-out on autophagy can be more directly observed. The above-mentioned results confirmed that PM2.5 inhibited the autophagy of bronchial epithelial cells, and the effect of IL-17A on autophagy can be further verified through a starvation model. The cells of IL-17A$^{-/-}$ mice witnessed increased LC3 expression (Figure 5F, G) and phosphorylation levels of PI3K, Akt, and mTOR (Figure 5H), yet reduced p62 expression (Figure 5F) compared with WT mice in a starvation model ($P < .05$). Therefore, PM2.5 could inhibit the level of autophagy by promoting the expression of IL-17A, which in turn activated the PI3K/Akt/mTOR signalling pathway in bronchial epithelial cells.

3.6 | PM2.5 promoted the secretion of IL-17A leading to the damage of mitochondrial function in airway epithelial cells

After PM2.5-induced model construction, the intracellular ROS level was increased in airway epithelial cells ($P < .05$, Figure 6A). Further investigation of mitochondrial morphology revealed that PM2.5 could promote mitochondrial division ($P < .05$, Figure 6B), increased DRP1 expression, decreased MFN2 expression ($P < .05$, Figure 6C) and ultimately reduced ATP biosynthesis ($P < .05$, Figure 6D). In addition, airway epithelial cells were extracted from both WT and IL-17A$^{-/-}$ mice after PM2.5-induced model construction to detect ROS level and ATP biosynthesis, the results of which showed that compared with the WT group, intracellular ROS level was decreased ($P < .05$, Figure 6E), and ATP biosynthesis was increased in the IL-17A$^{-/-}$ group ($P < .05$, Figure 6F). In summary, PM2.5 could impair the function of mitochondrial in airway epithelial cells via IL-17A secretion.
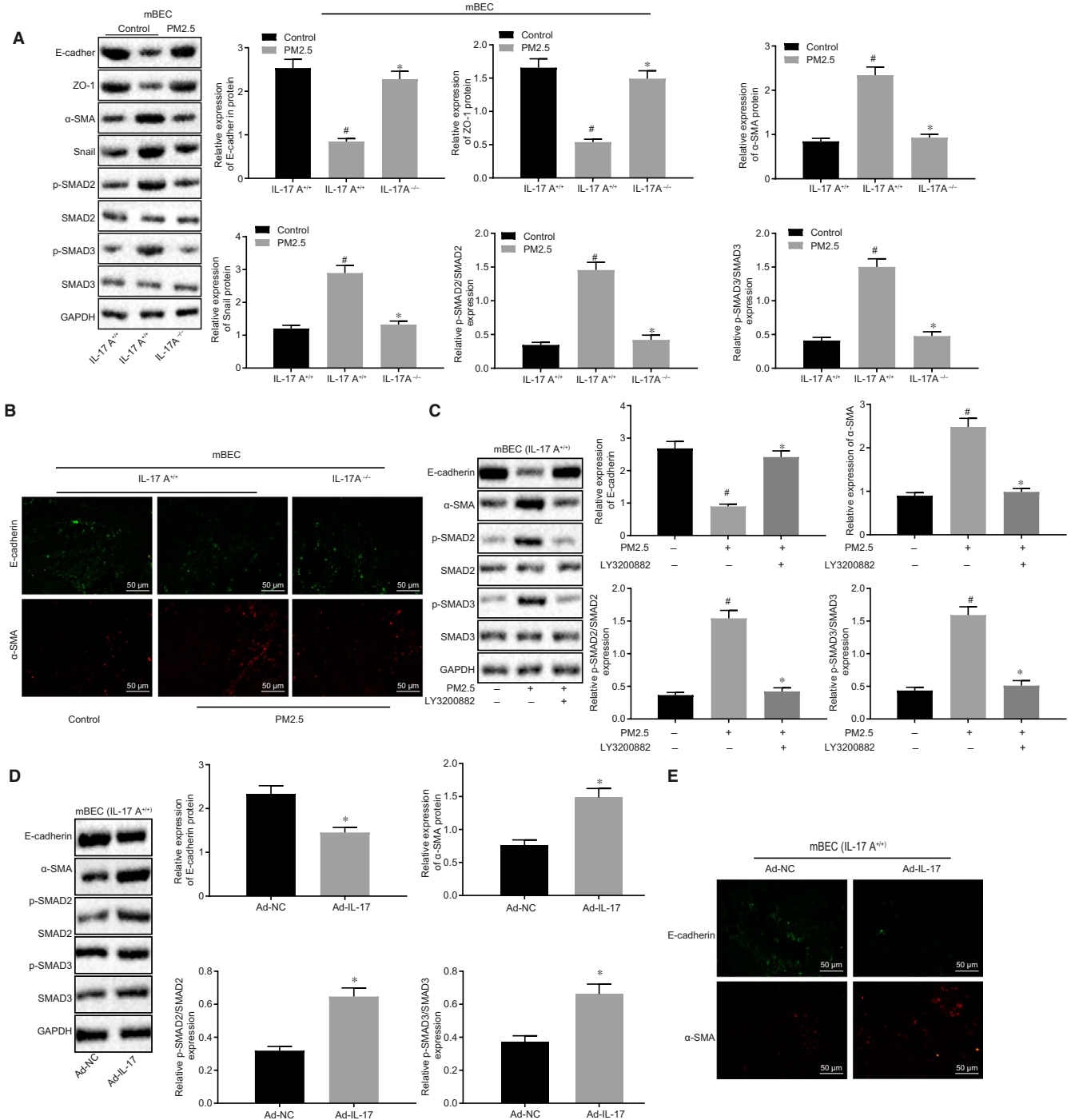
FIGURE 4 PM2.5 treatment produces IL-17A and activates the TGF signalling pathway, thereby resulting in pulmonary fibrosis. A, Western blot analysis of α-SMA, Snail, E-cadherin, ZO-1, SMAD2, p-SMAD2, SMAD3 and p-SMAD3 proteins in primary bronchial epithelial cells. The left represents representative protein bands, and the right represents a statistical chart. B, Representative images of immunofluorescence assay, green shows intracellular E-cadherin, and red shows α-SMA (×200). C, Western blot analysis of E-cadherin, α-SMA, SMAD2, p-SMAD2, SMAD3 and p-SMAD3 proteins in primary bronchial epithelial cells treated by LY3200882. D, Western blot analysis of E-cadherin, α-SMA, SMAD2, p-SMAD2, SMAD3 and p-SMAD3 proteins in bronchial epithelial cells upon IL-17A knockout treatment. The left panel represents representative protein bands, and the right panels represent statistical charts. E, Representative images of immunofluorescence assay, green shows intracellular E-cadherin, and red shows α-SMA (×400). *$P < .05$ vs IL-17A$^{+/+}$ mice following PM2.5 treatment; #$P < .05$ vs IL-17A$^{+/+}$ mice without PM2.5 treatment. Data (mean ± standard deviation) between two groups were compared using t test and those among multiple groups were assessed by one-way ANOVA with Tukey's post hoc test. Cell experiment was repeated 3 times
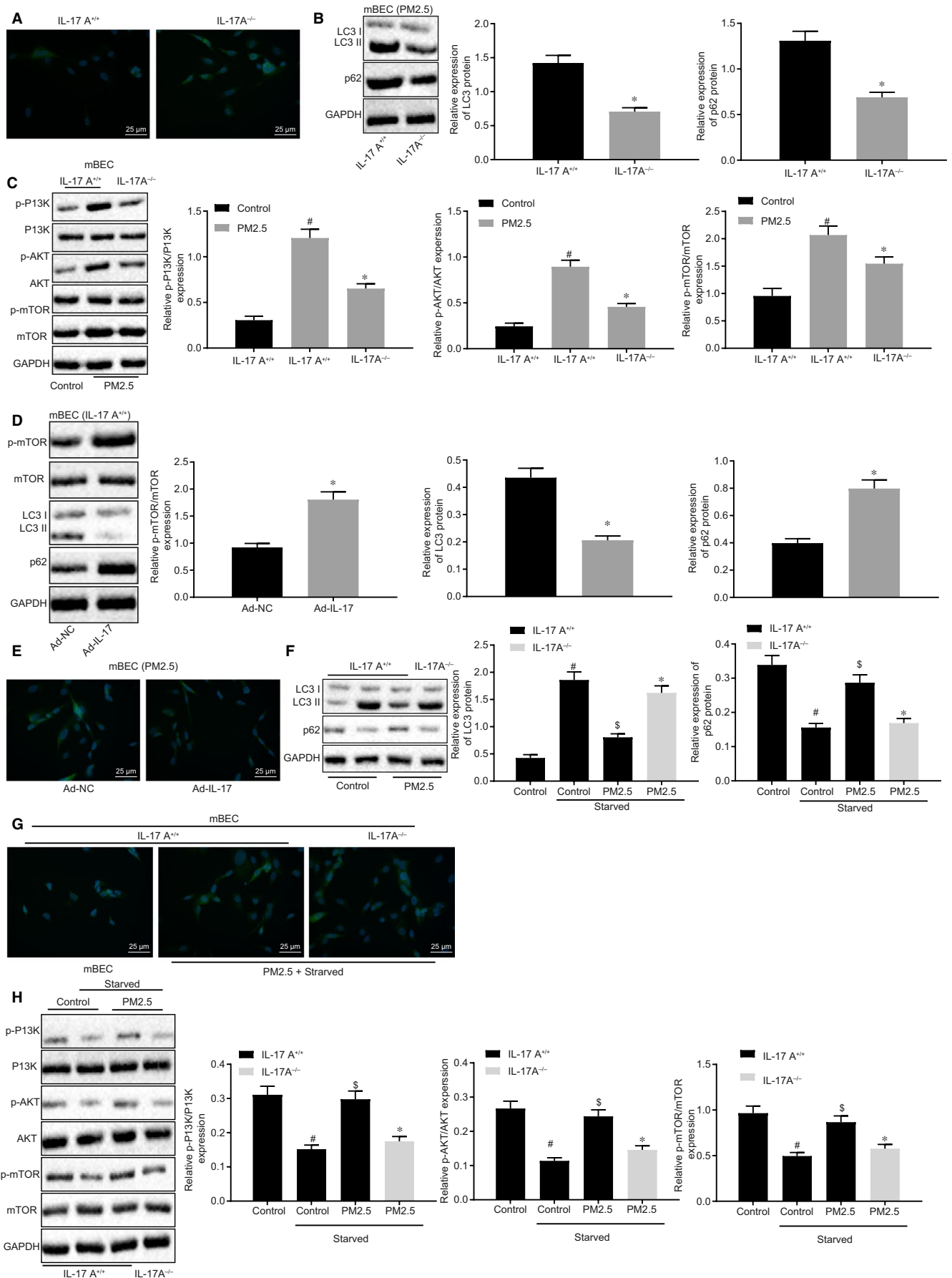
FIGURE 5 PM2.5 treatment inhibits autophagy by promoting IL-17A expression and activating the PI3K/Akt/mTOR signalling pathway in bronchial epithelial cells. A, Representative images of immunofluorescence assay (×400), green shows intracellular LC3, and red shows α-SMA. B, Western blot analysis of LC3 I, LC3 II and p62 proteins in mouse primary bronchial epithelial cells. *$P < .05$ vs IL-17A$^{+/+}$ mice following PM2.5 treatment. C, Western blot analysis of PI3K, p-PI3K, Akt, p-Akt, mTOR and p-mTOR proteins in mouse primary bronchial epithelial cells. *$P < .05$ vs IL-17A$^{+/+}$ following PM2.5 treatment. D, Western blot analysis of LC3 I, LC3 II, p62, mTOR and p-mTOR proteins in mouse primary bronchial epithelial cells. *$P < .05$ vs Ad-NC-treated mice. E, Representative images of immunofluorescence assay (× 400), green shows intracellular LC3, and red shows α-SMA. F, Western blot analysis of related proteins in mouse primary bronchial epithelial cells upon starvation. *$P < .05$ vs IL-17A$^{+/+}$ mice following PM2.5 and starvation treatment, #$P < .05$ vs IL-17A$^{+/+}$ mice without any treatment, $$P < .05$ vs IL-17A$^{+/+}$ following starvation treatment. G, Representative images of immunofluorescence assay (× 400), green shows intracellular LC3, and red shows α-SMA. H, Western blot analysis of related proteins in mouse primary bronchial epithelial cells. *$P < .05$ vs IL-17A$^{+/+}$ mice following PM2.5 and starvation treatment, #$P < .05$ vs IL-17A$^{+/+}$ mice without any treatment, $$P < .05$ vs IL-17A$^{+/+}$ following starvation treatment. Data (mean ± standard deviation) between two groups were compared using t test and those among multiple groups were assessed by one-way ANOVA with Tukey's post hoc test. Cell experiment was repeated 3 times
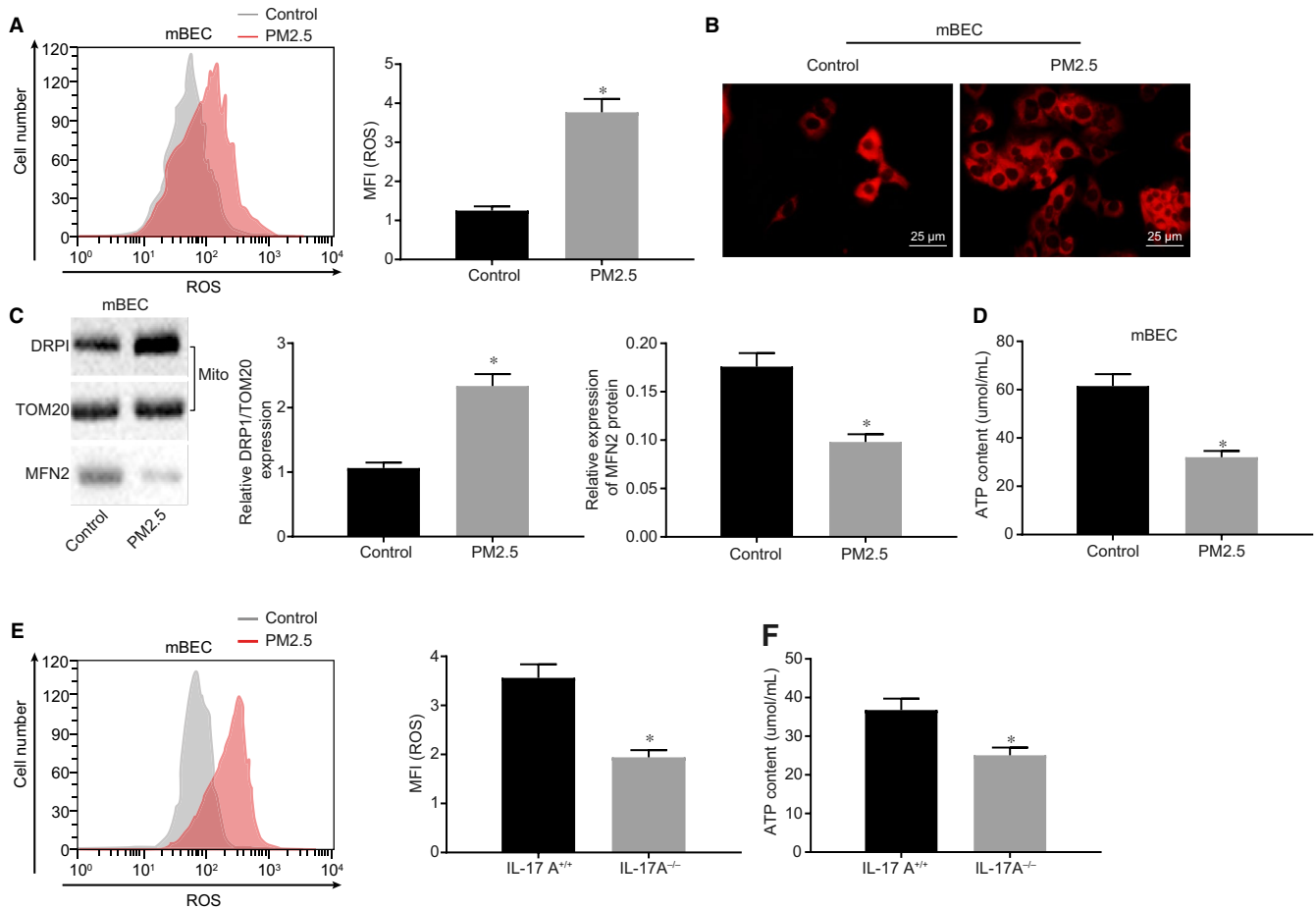

FIGURE 6 PM2.5 treatment promotes the secretion of IL-17A leading to mitochondrial damage in airway epithelial cells. A, Flow cytometry analysis of intracellular ROS content. B, Representative images of immunofluorescence assay (×400), red shows the mitochondria in the cells. C, Western blot analysis of DRP1, TOM20 and MFN2 proteins in mouse primary bronchial epithelial cells. D, Intracellular ATP content analysis. E, Flow cytometry analysis of intracellular ROS content. F, Intracellular ATP content analysis. *$P < .05$. Data (mean ± standard deviation) between two groups were compared using t test. Cell experiment was repeated 3 times

4 | DISCUSSION

In recent years, epidemiological data have revealed that cumulative ambient PM2.5 is associated with the morbidity and mortality of pulmonary and cardiovascular diseases, as well as cancer,[23] which brings an obvious social and economic burden. Especially, even a short-term enhanced PM2.5 concentration can contribute to increased mortality and morbidity.[24] Therefore, the present study was conducted to verify the cellular mechanisms underlying PM2.5 induced pulmonary inflammatory response and fibrosis in lung. Taken together, from the results presented here, it can be concluded that PM2.5 contributed to pulmonary inflammatory response and fibrosis via induction of IL-17A secretion.
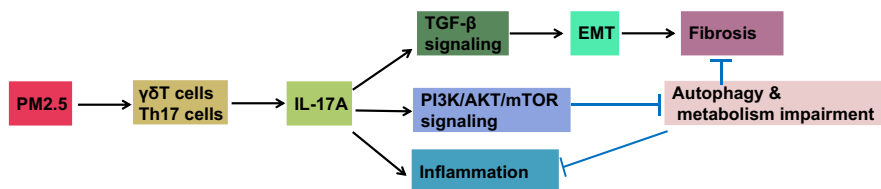
FIGURE 7 PM2.5 treatment promotes pulmonary inflammation and fibrosis by inducing secretion of IL-17A. PM2.5 inhibits autophagy of bronchial epithelial cells and promotes EMT by activating the TGF-β signalling pathway via the promotion of IL-17A secretion in γδT/Th17 cells, which ultimately aggravates inflammation and fibrosis

We firstly found that PM2.5 promoted the secretion of IL-17A in γδT/Th17 cells and aggravated the inflammatory response. It is known that there is abundant expression of IL-17A during the course of lung injury.[11,22] Evidence suggests that both γδT and Th17 cells secrete IL-17A to aggravate inflammatory response.[11,22] γδT cells are the highest producer of IL-17A in the early stages of infection and the Th17 cells are mainly responsible for protective effect of IL-17A.[22] Baldeviano et al found that IL-17A is able to stimulate the growth of dilated cardiomyopathy, and suppression of IL-17A reduces the myocarditis-induced cardiac fibrosis and also alleviates ventricular function.[25] Another study by Smith et al reported that the blockade of IL-17A activity decreases the incidence of atherosclerosis in ApoE2/2 mice,[26] and Wilson et al also demonstrated that BLM-mediated pulmonary fibrosis is dependent on IL-17A.[27]

Moreover, we also found that PM2.5 promoted the secretion of IL-17A, activated the TGF signalling pathway and promoted EMT in bronchial epithelial cells, thereby leading to pulmonary fibrosis. In agreement with our results, previous reports have also found IL-17A to be closely related with pulmonary fibrosis-related signalling pathways.[27-32] Moreover, the role of TGF-β is well known in migration, invasion as well as hyperplastic changes of lung fibroblasts in pulmonary fibrosis.[28,33,34] Consistent with our results, another study has reported that IL-17 mediated EMT through the induction of TGF-β1 and activation of the Smad2/3 and ERK1/2 signalling pathways.[31] Other researchers have also identified the production of EMT-related cytokines, chemokines and growth factors in pulmonary fibrosis, such as IL-17 [35] and TGF-β1,[36] which are significant for the development of pulmonary fibrosis.

Involvement of autophagy in pulmonary fibrosis injury has been described previously.[37] In addition, it has been reported that PM2.5 contributes to the suppression of autophagy in bronchial epithelial cells by inhibiting activation of the PI3K/Akt/mTOR signalling pathway.[14] Meanwhile, a literature confirmed that IL-17A can inhibit autophagy in keratinocytes by activating the PI3K/Akt/mTOR signalling pathway.[15] All these evidences support our findings that PM2.5 could inhibit the level of autophagy by promoting the expression of IL-17A, which in turn activated the PI3K/Akt/mTOR signalling pathway in bronchial epithelial cells. Apart from that, our study also found that PM2.5 promoted the secretion of IL-17A, leading to impaired mitochondrial function in airway epithelial cells. The function of mitochondria is very important in pulmonary fibrosis,[38,39] which is also related to EMT in alveolar epithelial cells.[40] Jin et al observed that PM2.5 results in disruption of mitochondrial structure via generation of reactive oxygen species, thereby leading to respiratory damage, which reveals a mechanistic foundation for the prevention of the outcomes in polluted environment.[41]

In summary, this study provides evidence that PM2.5 can inhibit autophagy and promote pulmonary inflammation and fibrosis by inducing the secretion of IL-17A in γδT and Th17 cells and regulating the PI3K/Akt/mTOR signalling pathway (detailed in Figure 7). An enhanced recognition of the effect of IL-17A lung injury improves our capability to seek for novel therapeutic interventions for those PM2.5-caused lung diseases.

CONFLICT OF INTEREST

The author declares no competing interest exists.

DATA AVAILABILITY STATEMENT

The data sets used and/or analysed during the current study are available from the corresponding author on reasonable request.

ORCID

Jun Duan https://orcid.org/0000-0003-3809-3065

REFERENCES

1. Jacono FJ, Mayer CA, Hsieh YH, et al. Lung and brainstem cytokine levels are associated with breathing pattern changes in a rodent model of acute lung injury. *Respir Physiol Neurobiol.* 2011;178:429-438.
2. Chu PY, Chien SP, Hsu DZ, et al. Protective effect of sesamol on the pulmonary inflammatory response and lung injury in endotoxemic rats. *Food Chem Toxicol.* 2010;48:1821-1826.
3. Goolaerts A, Pellan-Randrianarison N, Larghero J, et al. Conditioned media from mesenchymal stromal cells restore sodium transport and preserve epithelial permeability in an in vitro model of acute alveolar injury. *Am J Physiol Lung Cell Mol Physiol.* 2014;306:L975-985.
4. Cepkova M, Brady S, Sapru A, et al. Biological markers of lung injury before and after the institution of positive pressure ventilation in patients with acute lung injury. *Crit Care.* 2006;10:R126.
5. O'Toole TE, Hellmann J, Wheat L, et al. Episodic exposure to fine particulate air pollution decreases circulating levels of endothelial progenitor cells. *Circ Res.* 2010;107:200-203.

6. Shen Y, Zhang ZH, Hu D, et al. The airway inflammation induced by nasal inoculation of PM2.5 and the treatment of bacterial lysates in rats. *Sci Rep*. 2018;8:9816.

7. Zhou Y, Liu Y, Song Y, et al. Short-term effects of outdoor air pollution on lung function among female non-smokers in China. *Sci Rep*. 2016;6:34947.

8. Chen FP, Gong LK, Zhang L, et al. Early lung injury contributes to lung fibrosis via AT1 receptor in rats. *Acta Pharmacol Sin*. 2007;28:227-237.

9. Drakopanagiotakis F, Xifteri A, Polychronopoulos V, et al. Apoptosis in lung injury and fibrosis. *Eur Respir J*. 2008;32:1631-1638.

10. Li H, Du S, Yang L, et al. Rapid pulmonary fibrosis induced by acute lung injury via a lipopolysaccharide three-hit regimen. *Innate Immun*. 2009;15:143-154.

11. Mi S, Li Z, Yang HZ, et al. Blocking IL-17A promotes the resolution of pulmonary inflammation and fibrosis via TGF-beta1-dependent and -independent mechanisms. *J Immunol*. 2011;187:3003-3014.

12. Strieter RM, Mehrad B. New mechanisms of pulmonary fibrosis. *Chest*. 2009;136:1364-1370.

13. Ban GY, Pham DL, Trinh TH, et al. Autophagy mechanisms in sputum and peripheral blood cells of patients with severe asthma: a new therapeutic target. *Clin Exp Allergy*. 2016;46:48-59.

14. Liu T, Wu B, Wang Y, et al. Particulate matter 2.5 induces autophagy via inhibition of the phosphatidylinositol 3-kinase/Akt/mammalian target of rapamycin kinase signaling pathway in human bronchial epithelial cells. *Mol Med Rep*. 2015;12:1914-1922.

15. Varshney P, Saini N. PI3K/AKT/mTOR activation and autophagy inhibition plays a key role in increased cholesterol during IL-17A mediated inflammatory response in psoriasis. *Biochim Biophys Acta Mol Basis Dis*. 2018;1864:1795-1803.

16. Zhang S, Zhang W, Zeng X, et al. Inhibition of Rac1 activity alleviates PM2.5-induced pulmonary inflammation via the AKT signaling pathway. *Toxicol Lett*. 2019;310:61-69.

17. Wang X, Hui Y, Zhao L, et al. Oral administration of Lactobacillus paracasei L9 attenuates PM2.5-induced enhancement of airway hyperresponsiveness and allergic airway response in murine model of asthma. *PLoS One*. 2017;12:e0171721.

18. Li Q, Sun J, Chen X, et al. Integrative characterization of fine particulate matter-induced chronic obstructive pulmonary disease in mice. *Sci Total Environ*. 2020;706:135687.

19. Shaw AT, Maeda Y, Gravallese EM. IL-17A deficiency promotes periosteal bone formation in a model of inflammatory arthritis. *Arthritis Res Ther*. 2016;18:104.

20. Moroda M, Takamoto M, Iwakura Y, et al. Interleukin-17A-Deficient Mice Are Highly susceptible to toxoplasma gondii infection due to excessively induced T. gondii HSP70 and interferon gamma production. *Infect Immun*. 2017;85.e00399-17.

21. Bozinovski S, Seow HJ, Chan SP, et al. Innate cellular sources of interleukin-17A regulate macrophage accumulation in cigarette-smoke-induced lung inflammation in mice. *Clin Sci*. 2015;129:785-796.

22. Bai H, Gao X, Zhao L, et al. Respective IL-17A production by gammadelta T and Th17 cells and its implication in host defense against chlamydial lung infection. *Cell Mol Immunol*. 2017;14:850-861.

23. Jing Y, Zhang H, Cai Z, et al. Bufei huoxue capsule attenuates PM2.5-induced pulmonary inflammation in mice. *Evid Based Complement Alternat Med*. 2017;2017:1575793.

24. Liu Y, Wang L, Wang F, et al. Effect of fine particulate matter (PM2.5) on rat placenta pathology and perinatal outcomes. *Med Sci Monit*. 2016;22:3274-3280.

25. Baldeviano GC, Barin JG, Talor MV, et al. Interleukin-17A is dispensable for myocarditis but essential for the progression to dilated cardiomyopathy. *Circ Res*. 2010;106:1646-1655.

26. Smith E, Prasad KM, Butcher M, et al. Blockade of interleukin-17A results in reduced atherosclerosis in apolipoprotein E-deficient mice. *Circulation*. 2010;121:1746-1755.

27. Wilson MS, Madala SK, Ramalingam TR, et al. Bleomycin and IL-1beta-mediated pulmonary fibrosis is IL-17A dependent. *J Exp Med*. 2010;207:535-552.

28. Huang LS, Jiang P, Feghali-Bostwick C, et al. Lysocardiolipin acyltransferase regulates TGF-beta mediated lung fibroblast differentiation. *Free Radic Biol Med*. 2017;112:162-173.

29. Na M, Hong X, Fuyu J, et al. Proteomic profile of TGF-beta1 treated lung fibroblasts identifies novel markers of activated fibroblasts in the silica exposed rat lung. *Exp Cell Res*. 2019;375:1-9.

30. Vander Ark A, Cao J, Li X. TGF-beta receptors: In and beyond TGF-beta signaling. *Cell Signal*. 2018;52:112-120.

31. Wang T, Liu Y, Zou JF, et al. Interleukin-17 induces human alveolar epithelial to mesenchymal cell transition via the TGF-beta1 mediated Smad2/3 and ERK1/2 activation. *PLoS One*. 2017;12:e0183972.

32. Mack M. Inflammation and fibrosis. *Matrix Biol*. 2018;68–69:106-121.

33. Yue X, Shan B, Lasky JA. TGF-beta: titan of lung fibrogenesis. *Curr Enzym Inhib*. 2010;6,67-77

34. Oruqaj G, Karnati S, Vijayan V, et al. Compromised peroxisomes in idiopathic pulmonary fibrosis, a vicious cycle inducing a higher fibrotic response via TGF-beta signaling. *Proc Natl Acad Sci USA*. 2015;112:E2048-E2057.

35. Vittal R, Fan L, Greenspan DS, et al. IL-17 induces type V collagen overexpression and EMT via TGF-beta-dependent pathways in obliterative bronchiolitis. *Am J Physiol Lung Cell Mol Physiol*. 2013;304:L401-L414.

36. Dong Z, Tai W, Lei W, et al. IL-27 inhibits the TGF-beta1-induced epithelial-mesenchymal transition in alveolar epithelial cells. *BMC Cell Biol*. 2016;17:7.

37. Park S, Kim S, Kim MJ, et al. GOLGA2 loss causes fibrosis with autophagy in the mouse lung and liver. *Biochem Biophys Res Commun*. 2018;495:594-600.

38. Rangarajan S, Bernard K, Thannickal VJ. Mitochondrial dysfunction in pulmonary fibrosis. *Ann Am Thorac Soc*. 2017;14:S383-S388.

39. Kim SJ, Cheresh P, Jablonski RP, et al. The role of mitochondrial DNA in mediating alveolar epithelial cell apoptosis and pulmonary fibrosis. *Int J Mol Sci*. 2015;16:21486-21519.

40. Xu Q, Fang L, Chen B, et al. Radon induced mitochondrial dysfunction in human bronchial epithelial cells and epithelial-mesenchymal transition with long-term exposure. *Toxicol Res*. 2019;8:90-100.

41. Jin X, Xue B, Zhou Q, et al. Mitochondrial damage mediated by ROS incurs bronchial epithelial cell apoptosis upon ambient PM2.5 exposure. *J Toxicol Sci*. 2018;43:101-111.